

Subantarctic macrotidal flats, cheniers and beaches in San Sebastian Bay, Tierra Del Fuego, Argentina

Federico Vilas ^{a,*}, Alfredo Arche ^b, Marcelo Ferrero ^c, Federico Isla ^d

^a *Universidad de Vigo, Facultad de Ciencias, Dpto. de Geociencias Marinas y Ordenación del Territorio, Apto. 874, 36.200 Vigo, Spain*

^b *Instituto de Geología Económica, C.S.I.C.-U.C.M., Facultad de Geología, 28040 Madrid, Spain*

^c *Secretaría de Minería. Avda. de Santa Fé 1542, 1060 Buenos Aires, Argentina*

^d *CONICET, Centro de Geología de Costas y del Cuaternario, CC-722, 7600 Mar de Plata, Argentina*

Abstract

San Sebastian Bay is a large, semicircular coastal embayment situated on the Atlantic coast of Tierra del Fuego, Argentina. It is a high-energy, subantarctic environment with a tidal range of 10.4 m, influenced by large waves of Atlantic and local origin and swept by constant, strong westerly winds. A 17 km long gravel spit protects the Northern part of the Bay giving rise to a gradient in sedimentary processes. From south to north, are seven distinct sedimentary environments. Coastal sedimentation started at least 5200 years before present (BP) and a rapid progradation related to a relative sea-level drop has infilled about 6 kilometres of the Bay with a sedimentary sequence 10–11 m thick. 14-C dating of unabraded shells in the Chenier ridges of the relict part of the complex allows for a precise reconstruction of the stages of the progradation, that has slowed from 2.35 m/year at 5000 years BP to 0.6 m/year at present. The possible causes of the sea-level drop are discussed.

Keywords: Tierra del Fuego; macrotidal sedimentation; subantarctic climate; sea-level; glacio-isostatic rebound; chenier formation

1. Introduction

Macrotidal areas with tidal ranges over 8 m are relatively poorly studied in comparison with mesotidal (range 2–4 m) areas. Some of them are estuarine in character, such as the Severn River (UK) (Kirby and Parker, 1982; Harris and Collins, 1985; Allen, 1987, 1988, 1990), Seine Estuary–Mont Saint Michel (France) (Larsonneur, 1982; Avoine, 1986; Avoine and Larsonneur, 1987), and the Bay of Fundy (Canada) (Knight and Dalrymple, 1975; Amos et al.,

1980; Dalrymple et al., 1990), among others. Some other well known examples are dominated by marine tidal processes such as the Wash (UK) (Evans, 1965) and Jade Bay (Germany) (Reineck, 1958, 1972), Taizhou Bay (China) (Ren, 1986), Bohai Sea (China) (Wang, 1983) and Inchon Bay (Korea) (Frey et al., 1988, 1989).

In the Southern Hemisphere, macrotidal areas are even less well known even though the tidal ranges and tidal flats at the Atlantic mouth of the Magellan Strait and the Atlantic Coast of Tierra del Fuego are among the largest in the world. The authors conducted surveys of San Sebastian Bay (Fig. 1) between 1985 and 1988 aimed at characterising the

* Corresponding author. Fax: +34-8681-2556; E-mail: fvilas@uvigo.es

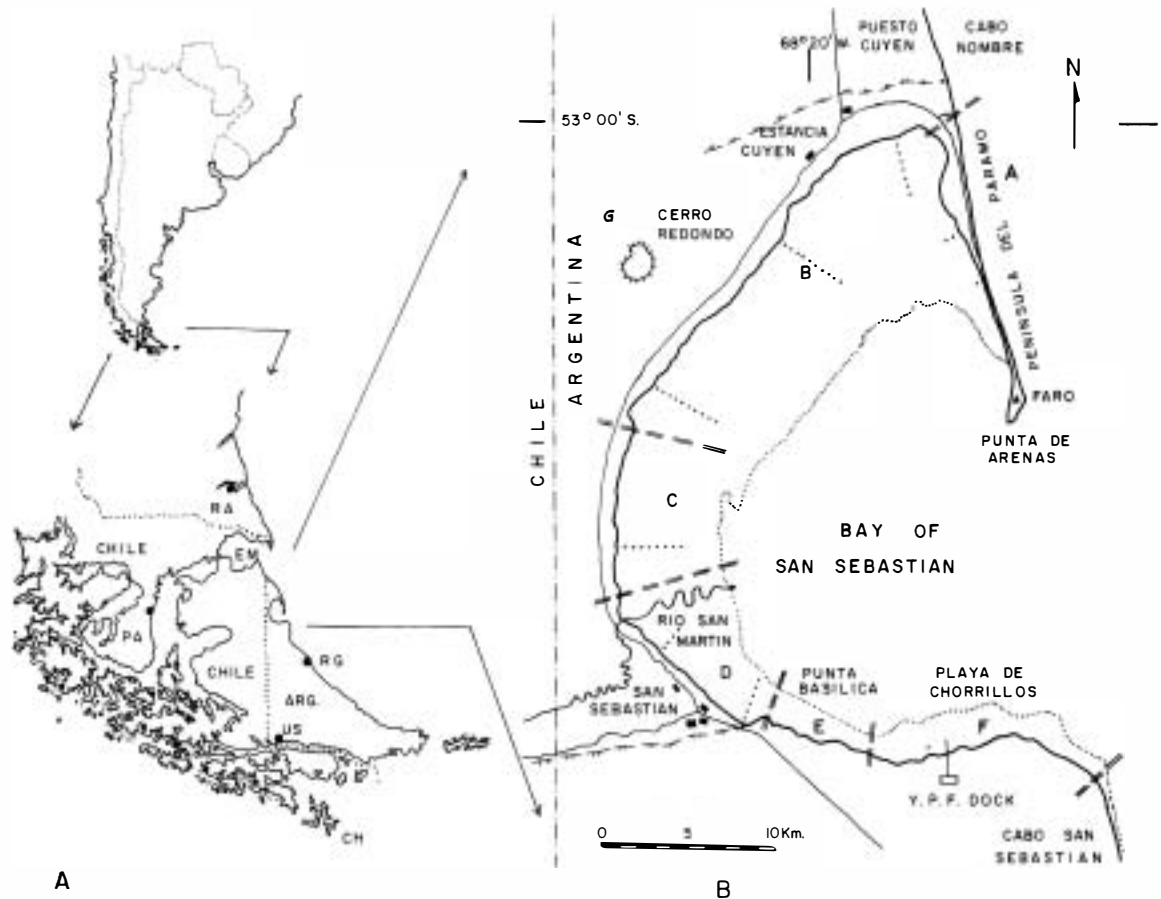


Fig. 1. (A) Map of situation. (B) The Bay of San Sebastian and different physiographic sectors (A to G). Dotted lines are surveyed profiles sampling stations. RG: Río Grande, RA: Río Gallegos, PA: Punta Arenas, EM: Strait of Magellan, CH: Cape Horn, US: Ushuaia. Location of profiles shown in Fig. 15 are indicated.

sedimentary subenvironments, sedimentary processes, sequences, and the Quaternary evolution of the area.

The Bay presents an interesting combination of physiographic features: extreme macrotidal regime, high latitude, subantarctic climate, fine-grained sedimentation in a high-energy environment and related wave- and wind-dominated areas. The bay could provide an alternative example to the classic areas listed above and some guidance for the interpretation of ancient, fine-grained, marine deposits.

The San Sebastian Bay area exhibits a series of features which could be interpreted as representing a Holocene fall of sea level of eustatic and/or isostatic origin, such as raised beaches and chenier ridges,

most of them rich in organic remains, allowing for C-14 dating. The quantification and interpretation of the sea-level fall and its causes was another goal of our research.

2. Location

2.1. Geographic setting

San Sebastian Bay is a coastal embayment situated in the North of the Argentinean territory of the Isla Grande de Tierra del Fuego (Fig. 1); it lies between 63° 40' and 63° 48' long. W and 53° 00' and 53° 25' lat. S.

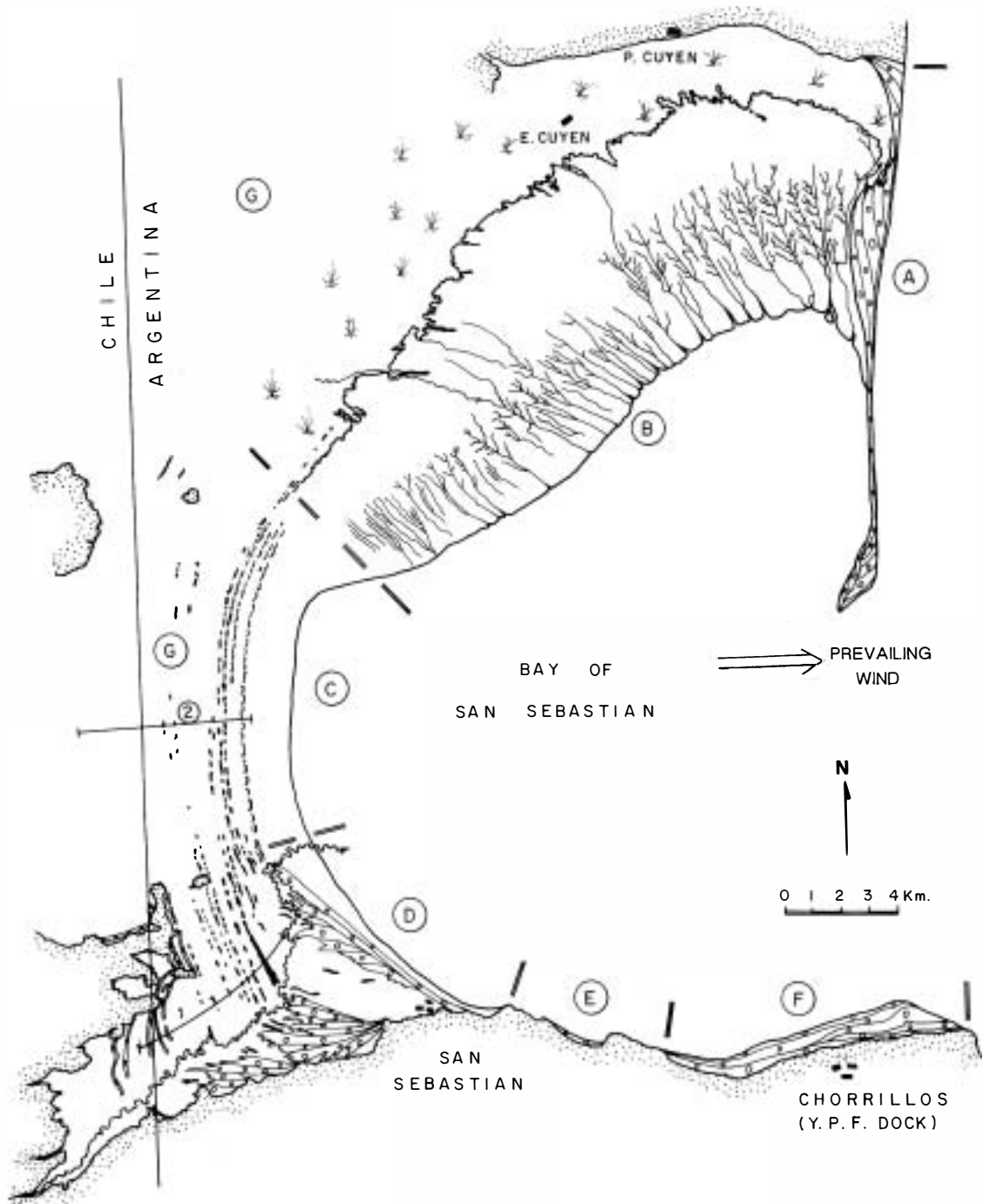


Fig. 2. Map of the Bay. (A) Gravel beaches of Península del Páramo, (B) Muddy tidal flat with tidal channels, (C) Cheniers and muddy tidal flat without tidal channels, (D) Beach complex of San Sebastian, (E) Cliffs of Punta Basílica, (F) Barrier Beach-Lagoon Complex of Chorrillos, and (G) Fossil sediments deposited during Holocene times. 1 and 2 are the surveyed profiles represented in detail in Fig. 16.

The Bay is roughly semicircular in shape, measuring approximately 40 km from north to south and 25 km from east to west (Fig. 2). Astronomic tides range from 3.4 m to 10.4 m (Servicio de Hidrografía Naval, 1987, 1988). The average rainfall is 300–320 mm/yr, the prevailing wind comes from the west, exceeding 60 km/h for more than 200 days per year, with occasional gusts up to 155 km/h, the stability of the cyclone patterns in the subantarctic region (50° to 65° lat. S) is responsible for the small variation of wind direction. Maximum summer temperatures reach 16°C–18°C, while in winter minimum temperatures of –20°C occur frequently with periods of several months when the average temperature is below 0°C and the sea water freezes (Servicio de Meteorológico Nacional, 1986).

2.2. Geologic setting

The bedrock of the area is the Miocene Carmen Silva Formation (Codignotto and Malumian, 1981) consisting of deltaic fine sands and silts. It was deeply eroded during the first and largest Patagonian Glaciation (Caldenius, 1932) by a glacier coming from the Patagonian Iceshield, flowing to the NE from Dawson Island and eroding in the last 15,000 years the Inútil Bay (Chile)–San Sebastian Bay (Argentina) depression. A later, Pleistocene glacial period took place in the area and the Tapera Sur Till was deposited (Codignotto, 1979, 1983). Submerged moraines at a depth of 5 m have been recognised in the shelf, NE of San Sebastian Bay (TOTAL AUSTRAL-GEOMATTER, 1980).

Raedecke (1978) made reference to several moraine systems, located between Bahía Inutil and Bahía de San Sebastian and their possible succession and Codignotto and Malumian (1981) compiled the geology of the Northern Tierra del Fuego and mentioned the ‘rhythmic topography’ of the Holocene sediments in the San Sebastian Bay area.

More recent research work was specifically aimed at establishing the succession of glacial and interglacial periods, the stratigraphy of moraines and coastal sediments and present-day sedimentary pro-

cesses and rates of sedimentation in the area. Porter et al. (1984) described the Holocene sea level fluctuations in the Magallanes–Beagle region, Heusser and Rabassa (1987) described and interpreted the climatic changes and glacial retreat stages in the last 12,000 years in the same area and Rutter et al. (1989) correlated the Quaternary deposits along the Patagonian and Fuego coastline.

Vilas et al. (1987) and Isla et al. (1991) described the main sedimentary sequences, the sediment source areas and the winter and summer wave regimes in San Sebastian Bay that occur in two areas with different characteristics: (1) a wave-dominated gravel spit and (2) a tide-dominated mud flat. Bujalesky et al. (1987) described the Páramo Peninsula gravel spit, and Isla (1993) described the gravel segregation and armouring processes in the Páramo Peninsula, and the coastal spit that partially closed San Sebastian Bay.

The Bay is flanked to the north and the south by cliffs which at present are undergoing erosion; the northern cliffs are composed of Pleistocene Tills, whereas the southern ones comprise the fine-grained, siliciclastic, Miocene Carmen Silva Formation. Sedimentation occurs in two areas with very different characteristics (Fig. 2): the Peninsula del Páramo (Zone A), composed of gravel beaches, and the inner coast of the Bay (Zones B–F), where muddy tidal flats and sand–gravel beaches are found. As these sedimentary environments prograded seawards during the Holocene, these coastal sediments covered most of the much wider original San Sebastian Bay to the west, and extensive eolian deposits cover most of the Holocene deposits.

This paper deals with the sedimentary processes and deposits of the intertidal area (Fig. 2, Zones B to F). The sedimentology of the Peninsula del Páramo Spit (Fig. 2, Zone A) has been discussed previously by Isla et al. (1991).

3. Research methods

The different subenvironments required specific research methods according to their dynamics and

Fig. 3. (overleaf) Several aspects of the intertidal area north of the Bay. (A) Straight main tidal channel, (B) Sinuous secondary tidal channel, (C) Spiderweb structure, (D) View across a main tidal channel.

A



B





grain size. Two methodologies were employed, one for tidal flats and another for sandy and gravel beaches.

Seven profiles were established by surveying on the tidal flats of the Bay (Fig. 1B). The survey was carried out using a theodolite Kern BKM-1. At each station the sediments were sampled for biota, grain-size, radio carbon dating, and mineralogical analysis by means of Senckenberg boxes and/or, 6 cm diameter by 40 cm PVC tubes.

Along three of the main tidal channels, water samples were collected using 1 l plastic bottles on poles left during low tide to measure the suspended matter. Wooden reference stakes were planted and their distance to the edge of the channel measured each summer to determine channel migration rates.

The size distribution granulometry of the silt-clay fraction of the sediments was determined by settling tube and SEDIGRAPH. Mineralogy was determined by X-ray diffraction. Photographs were taken of 26 cores to observe internal structures.

A series of fixed stations spread 1 km apart were surveyed in the beach ridges near San Sebastian (Fig. 2, Zone D) above the spring high water mark. They served as a reference base for the summer beach profiles, gravel sediment sampling and for imbrication measurement of the *a-b* axis planes. The geomorphic and sedimentary features of the Península del Paramo and San Sebastian beach complexes were mapped at 1:20,000 scale and a 1:40,000 map of the recent and Holocene tidal and beach sediments of the Bay area was compiled after terrain observations and aerial photograph interpretation.

4. Results: sedimentary environments, processes, facies and sequences

Sedimentation presently occurs in two areas (Fig. 2): the Península del Paramo (Zone A), a gravel spit (out of the scope of this paper), and Intertidal part of the Bay of San Sebastian, in which several subsystems can be distinguished: a muddy tidal flat (Zone B), a chenier coast facing a narrower tidal flat (Zone C), a gravel-sand beach near San Sebastian (Zone D), the cliffs of Punta Basilica (Zone E) and the barrier-lagoon complex of Chorrillos (zone F). Similar relict sediments extend westwards (Zone G),

deposited during the Holocene in a phase of active coastal progradation and partly covered by eolian deposits, marshes and peat bogs.

4.1. The northern muddy tidal flat (Fig. 2, Zone B)

During spring low water periods, an area 7-10 km wide and 21 km long (approx. 185 km²) is exposed subaerially in the north part of the Bay. Intertidal flat sediments consist of grey-green silts and clays. The flats can be subdivided, from top to base into: (1) the *supratidal zone*, always above seawater level, partially or totally vegetated; (2) the *upper intertidal zone* flat, almost featureless, devoid of vegetation and exposed subaerially several days during neap tides, with some periglacial structures; (3) the *middle intertidal zone*, with permanent, elongate seawater pools exposed at low tide, orientated E-W by the action of dominant winds; and (4) the *lower intertidal zone*, with dendritic, sinuous and straight tidal channels.

The strong west winds, up to 55 km/h (Servicio de Metereológico Nacional, 1986), force waters eastward and amplify ebb currents locally (Servicio de Hidrografía Naval, 1987). Long period oceanic waves are refracted to the south and their action is negligible in the northern part of the Bay (Isla et al., 1991); the Península del Paramo deflects ebb currents to the south-southeast.

4.1.1. Supratidal zone

The supratidal zone is defined here as the area where halophytes are in the minority of the total plant species present or totally lacking (Beefnik, 1977; Frey and Basan, 1985). Plants such as *Salicornia*, *Lepidophyllum* and several species of Gramineae colonize the supratidal area. The vegetation disappears seawards except for circular mounds of *Salicornia*. Supratidal sediments are grey-green mud with faint parallel lamination and many rootlet horizons. Brackish conditions are frequent because of salt spray delivered by strong winds and occasional dissolution of ephemeral salt crusts by rainwater.

4.1.2. Upper intertidal zone

The upper intertidal zone is a flat area, devoid of vegetation, 800 m wide. It is pervasively mud-cracked as it is submerged only during springs. The

sediments are grey–green mud, well laminated, with infilled mud cracks.

A characteristic surface structure of this area (Fig. 3C), is a radial and concentric ‘spiderweb’ association of closely spaced mudcracks forming depressions a few millimetres deep and 50–80 cm wide. The fabric of the sediments is chaotic (not laminated) up to 6 cm below the structure. It has been interpreted as a periglacial feature caused by repeated freezing and thawing of water collected in small depressions. During neap tide periods of the summer, ‘spiderweb’ structures are absent and mudcracks develop in a different pattern, in response to the difference of internal structure of the sediments under this area and the normal, laminated sediments.

4.1.3. Middle intertidal zone

This zone is about 600 m wide. Water remains here in places after the tide retreats forming elongate shallow tide-pools up to 15 cm deep, 40–50 cm wide

and several meters long, orientated E–W subparallel to the prevailing wind direction: their size increases seawards. Algal mats grow at the bottom of the pools and trap fine sediment during slack water periods. The rest of the area is flat and covered by mud cracks. Polychaete worms live in vertical U-tubes mostly associated with the tide-pools.

Sediments in this zone are well laminated, with grey silt and black clay laminations. The latter correspond to rotting algal mats and diatom films.

4.1.4. Lower intertidal zone

This is the most extensive zone in the study area, and is 5–7 km wide, characterised by numerous tidal channels (Fig. 3A,B). The channels develop by coalescence of the tide-pools under wind action, evolving seaward into small, highly sinuous channels and finally to deep, straight channels (Fig. 4). The length and width of the channels increase in a seawards

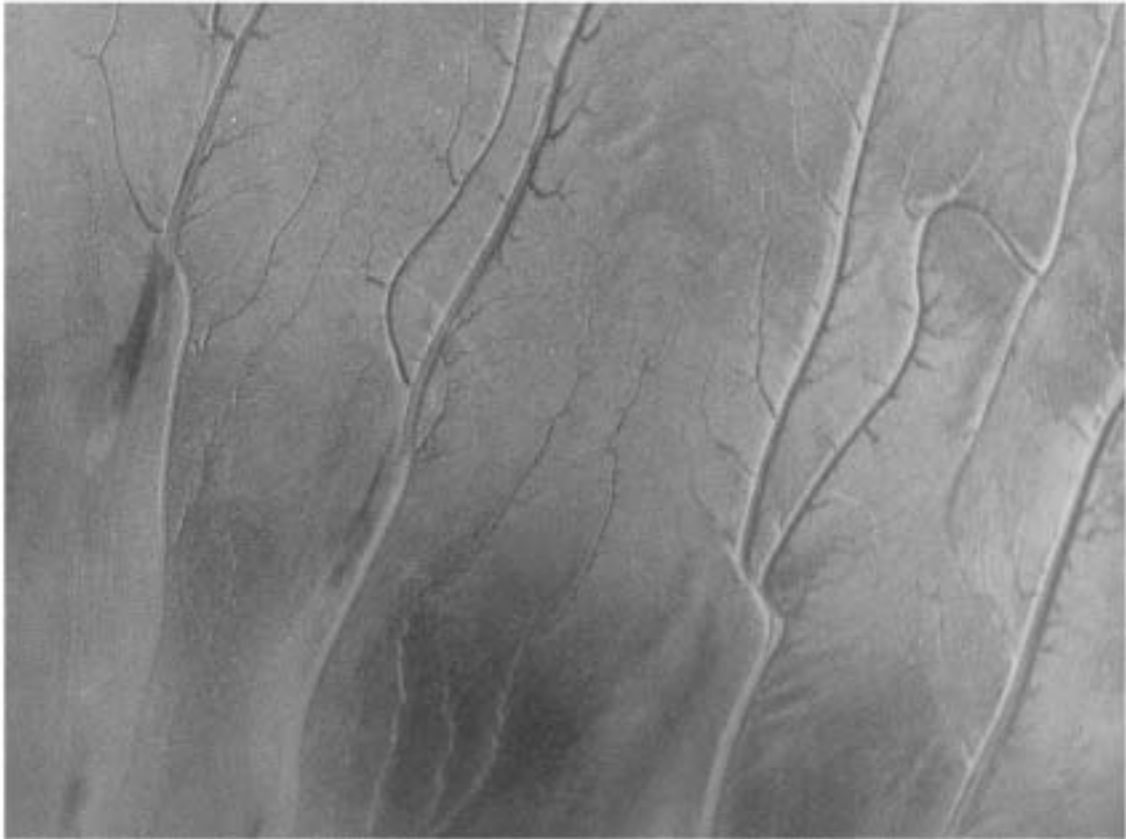


Fig. 4. View of a capture process, in an aerial photograph.

direction. Channel capture processes are frequently observed (Fig. 5) among tidal channels.

The sediments consist of silts and clays, dark grey in colour with an organic matter content of 0.9% to 1.9%, principally derived from algal films. The main internal structures are parallel lamination, lenticular bedding and large-scale lateral accretionary surfaces. Sedimentation takes place both in the channels and the interchannel areas.

The only macrofauna living in the area are mature polychaete worms, living in U-shaped tubes that can heavily disturb the original lamination. Diatoms are also very common, covering the surface of the sediments with a rusty coloured film. Amphipods are present in the lower reaches of the tidal channels.

Channels are initiated when tide-pools merge into parallel rills by the erosive action of wind induced wavelets at the far end of each pool. As water flows downslope (and gravity exceeds the wind effect), the rills develop a high-sinuosity configuration and mi-

grate laterally, forming point bars with accretionary surfaces dipping at 16° – 24° and a basal lag of rounded, imbricated clay chips (Fig. 3D).

The sinuous channels coalesce seawards to form straight channels of asymmetric, triangular cross-section up to 20 m wide and 3.5–4 m deep (Fig. 3A). They flow almost parallel to each other and have funnel-shaped mouths (Fig. 4). They migrate to the east and have an erosive, almost vertical east bank and an accretionary western bank dipping 17° – 24° . Channels bed are usually flat covered by imbricated (landward dipping) clay chips, immersed in a very fluid clay–water mixture. The internal structure of the channel deposits comprise large-scale lateral accretionary surfaces, dipping to the E or NE.

Tributary channels cut across the interchannel banks. Those trending across an accretionary bank are almost straight, developing microdeltas at the mouth, but those running across an erosive bank are highly sinuous, with higher slopes and larger mi-

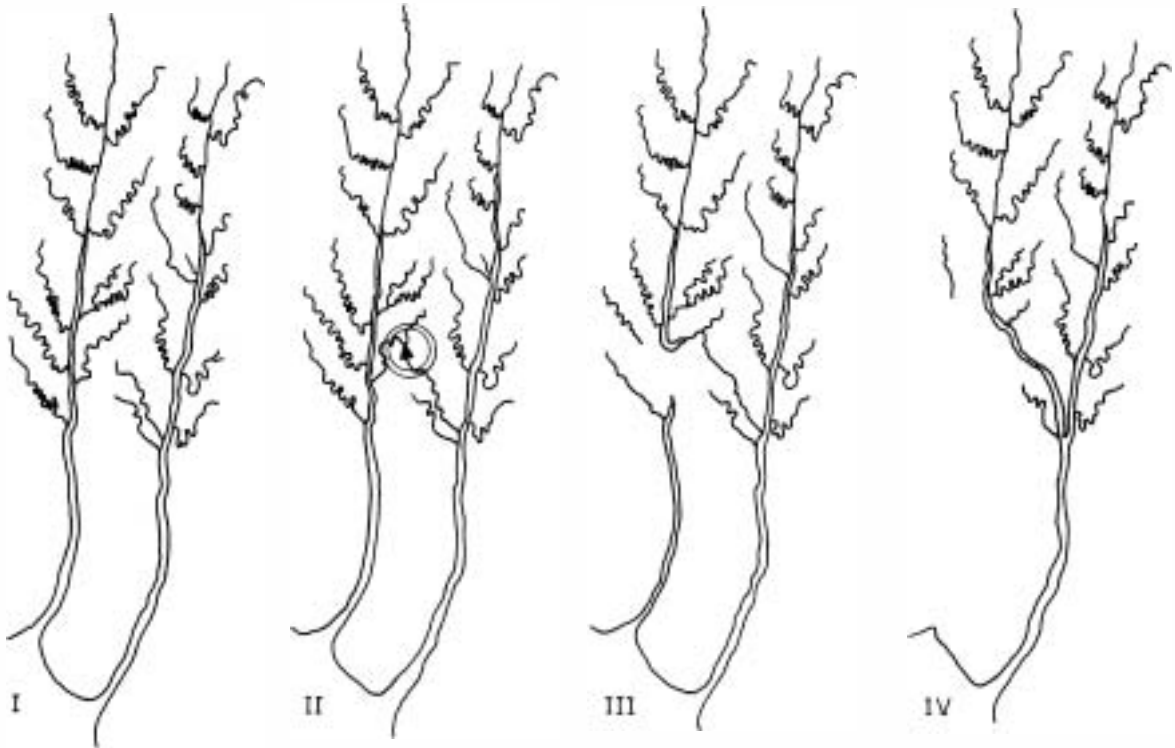


Fig. 5. Capture or piracy processes are frequent among tidal channels; (I) Initial stage, (II) A secondary channel captures the upper part of a neighbour channel, (III) The lower part of the captured channel is abandoned and infilled, and a sharp angle is formed in the capture zone. (IV) In a mature stage, the bend straightens up and only relics of the former lower channel system remain.

croddeltas. Rotational slumps are common in erosive banks, modifying the main channel trace (Fig. 3A).

Segments of the tributary channels that become abandoned by avulsion and capture are infilled by fines falling out of suspension during high-water slack periods. The resulting channel-fill deposits have a lenticular geometry, an erosive base characterised by imbricated clay chips and concave upwards bivalve shells, reflecting the progressive infilling of the channel.

4.1.5. Mineralogy and grain size of the northern muddy tidal flat sediments

X-ray diffraction shows that the mineralogy of the clay fraction of intertidal sediments is characterised by between 44% and 73% chlorite, 20% and 32%

illite and 7% and 29% smectite. Two possible sources of the intertidal mud are the matrix of the tills located to the north of the Bay or the miocene outcrops found to the south of the Bay. The till matrix has a mean composition of 13% chlorite, 21% illite and 66% smectite, very different from the intertidal sediments; this fact and oceanographic data discussed below exclude the tills as a significant source of fine sediments to the Bay.

The clay mineralogy of the fine fraction of the Miocene rocks of the southern part of the Bay is characterized by chlorite (55–75%), illite (20–25%) and smectite (10–28%); these values are very close to those of the intertidal sediments.

The grainsize data discriminates two domains: the intertidal area, with percentages of sand that seldom

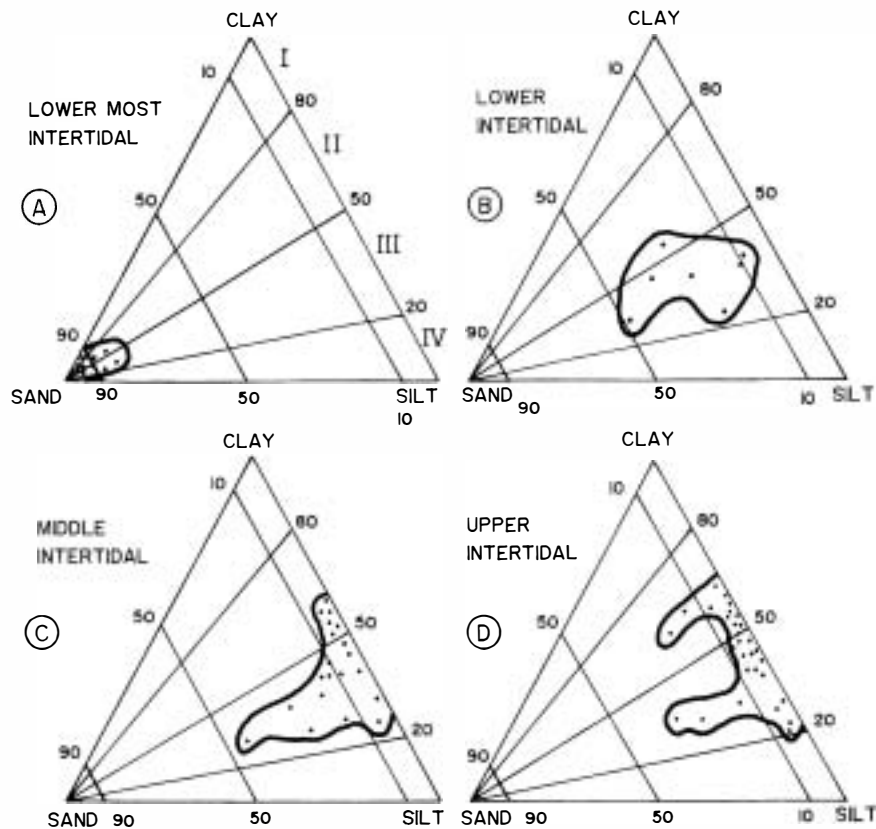


Fig. 6. Granulometric characteristics of the sediments represented in a Pejrup (1988) diagram; I to IV represent domains with increasing energy conditions. (A) Lowermost intertidal domain; this is the most energetic and clays and silts are kept in suspension. (B) Lower intertidal domain; lower energy reflected by a sand content less than 50%. (C) and (D) Middle and upper intertidal domains; the less energetic parts of the complex, dominated by fine sediments. The coarsest samples collected in channels and rills.

exceed 10% for the upper and middle part and 50% for the lower part and the lowermost edge of the intertidal zone, with 90% of fine sand (Fig. 6). The increase in sand content towards the lower intertidal zone could be attributed to increased tidal current velocities. The dominance of sand fraction in the lower zone reflects a change in the dominant current and energy associated with the passage from a channelled domain (intertidal area) to a non-channelled (subtidal) regime (Fig. 6A).

The intertidal zone to the north of San Sebastian Bay exhibits a remarkably small grainsize variation from top to base (silts and clays usually in excess of

90%), in spite of the strong tidal currents of the area and occasional high wave regime; these high-energy conditions are the cause of most samples been plotted in domain III (see Fig. 6).

4.1.6. Sedimentary sequences

Small-scale internal structures are difficult to observe in natural outcrops or trenches because of the muddy nature of the sediments, but can be seen in the X-ray images of the undisturbed cores (Fig. 7). Parallel lamination, current ripples and lenticular bedding are the only structures present, together with vertical tubes (*Arenicolites* type Fig. 7B,D,F).

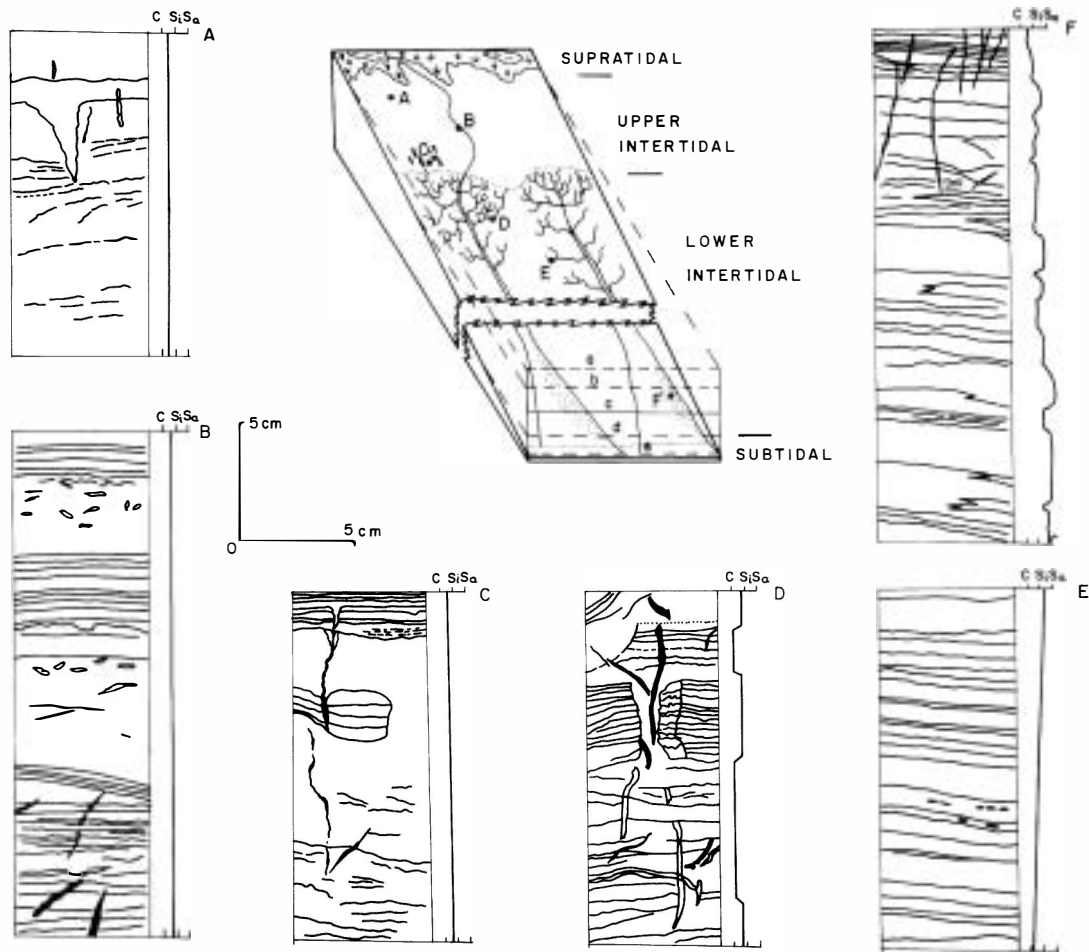
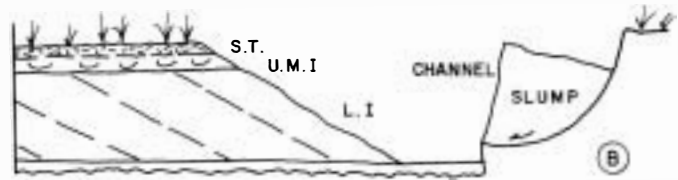
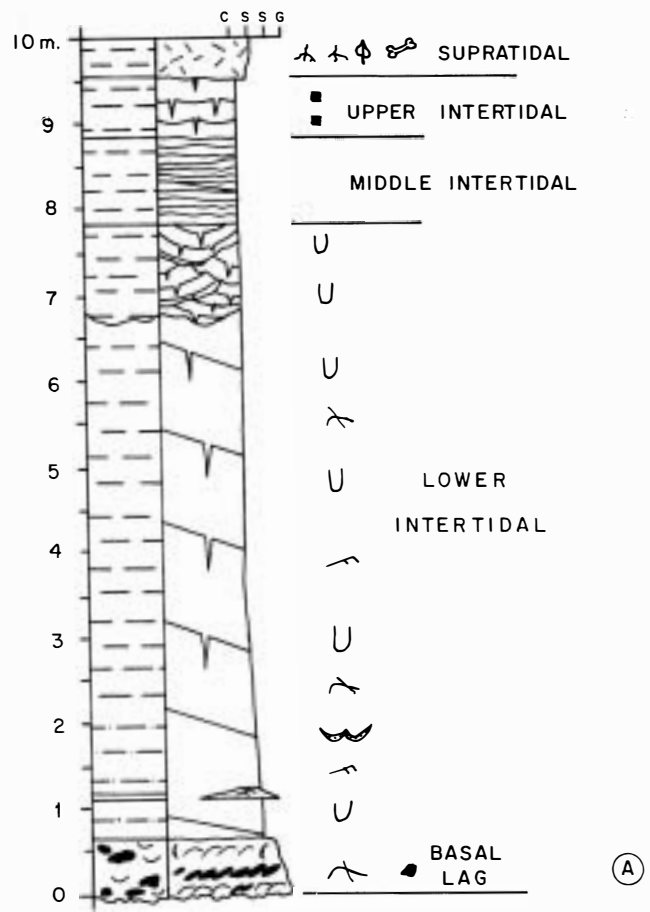


Fig. 7. Selected line drawings of internal structures of the intertidal sediments from X-ray images of short cores. Parallel lamination, current ripples and bioturbation are the only structures observed, and the high energy of the area is not reflected in the internal structures. C: clay, Si: silt, Sa: sand. Deformed horizontal tubes are present in B and E sediments.



- | | | | |
|--|--------------------|--|--------------------------|
| | ROOTLETS | | CURRENT RIPPLES |
| | PLANT REMAINS | | CLAY CHIPS |
| | VERTEBRATE BONES | | PEBBLES |
| | BIOTURBATION | | MUD CRACKS |
| | BROKEN BIVALVS | | PARALLEL LAMINATION |
| | BROKEN GASTROPODES | | LARGE-SCALE CROSSBEDDING |
| | RODENT BURROWS | | FLASER BEDDING |
| | | | LINSEN BEDDING |

Fig. 8. (A) Active tidal channel sequence, reconstructed after field observations. (B) Lateral migration of the tidal channels towards the east, forming prominent lateral accretion surface.

The lateral succession of sedimentary facies observed in the field and in the short cores were integrated according to Walther's Law to deduce a facies succession for the Northern Muddy Tidal Flat (Fig. 8). It is about 10 m thick and can be subdivided into four parts.

–Supratidal zone: 0.3–0.4 m thick, mudcracked silts and clays, eolian silts and granules, abundant rootlets and vegetal fragments. Faint, parallel lamination or massively bedded occasional vertebrate bones.

–Upper intertidal zone: 0.6–0.7 m thick, parallel laminated, mudcracked silts and clays, sometimes

massive due to repeated desiccation–dampening periods. Occasional halite crusts a few millimeters thick.

–Middle intertidal zone: 0.8–1 m thick, similar to the previous one in grain size and internal structures, polychaete worm tubes appear here and increase in size and diameter towards the lower intertidal zone.

–Lower intertidal zone: about 8 m thick. It consists entirely of channelled muddy sediments. At the top, lenticular bodies of uncracked silts and clays, with concave surfaces, followed by thick tabular bodies of similar grain size with lateral accretion

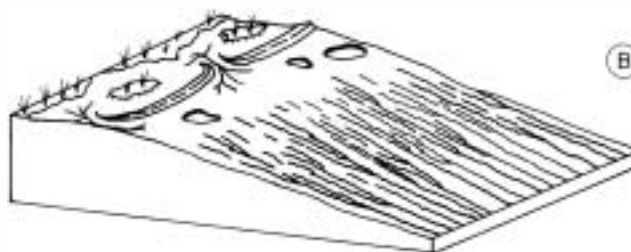
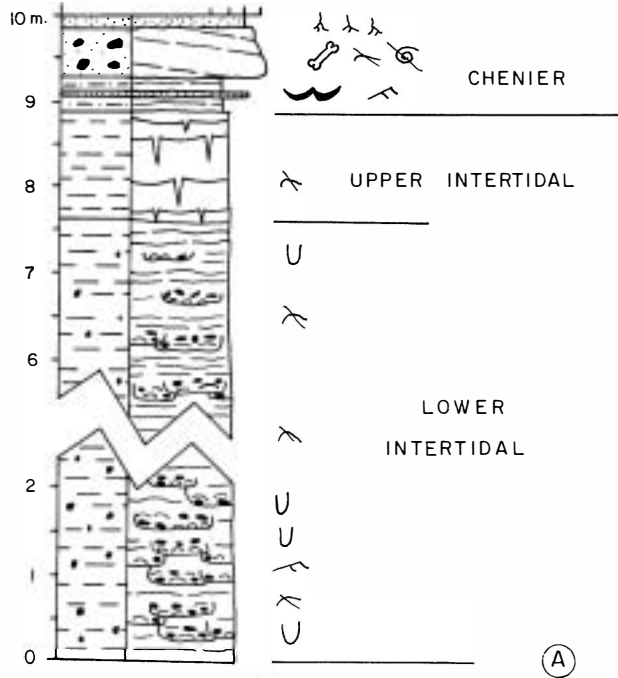


Fig. 9. (A) Chenier-Tidal flat sequence. (B) Diagram (not to scale) of the lateral relationships between cheniers, wave-erosion puddles and rills. For legend see Fig. 8.

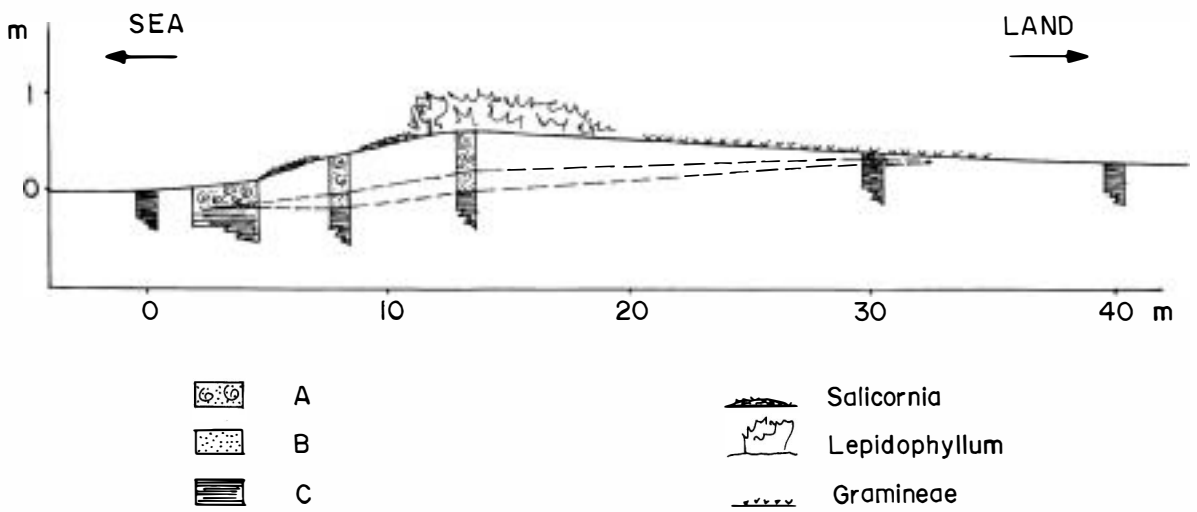


Fig. 10. Section of a chenier ridge as seen in shallow trenches. (A) Chaotic accumulation of Bivalves and Gastropods in a silt-day matrix. (B) Sands and silts with flaser bedding and parallel lamination. (C) Intertidal mudflat sediments. Also shown are the most typical plants of the ridges.

surfaces, sometimes mud cracked. A lag layer of shell debris and clay chips in a clay matrix occurs at

the base. The sequence must lie on an erosive surface representing the bottom of the channels, but this



Fig. 11. Rills or incipient channels, East of Cerro Redondo. It is a wind-driven drainage network consisting of hundreds of similar, parallel furrows.

has not been observed directly. Some fine sand lenses are found occasionally.

4.2. Cheniers and mudflats (Fig. 2, Zone C)

This sector is 13 km long and 4–5 km wide. During low tide an area of approximately 65 km² is exposed. Fig. 10B shows a drawing of the chenier flat formation and Figs. 8 and 9A give a vertical sedimentary sequence. Three distinct areas can be differentiated.

–Supratidal zone, comprising chenier ridges colonised by plants including *Lepidophyllum*, *Salicornia* and different Gramineae. Seawater reaches the area once or twice a year when spring tides coincide with large SE storms.

–Upper intertidal zone: a flat, featureless area, mudcracked with muddy sediments.

–Lower intertidal: a muddy area with parallel, wind-controlled rills, grading seaward into a sand flat near the low-water spring tide mark.

4.2.1. The supratidal zone (chenier plain)

The supratidal zone exhibits flats and narrow ridges parallel to the coastline with curved ends, 0.7–0.9 m high, 120–600 m long and spaced sepa-

rated 80–350 m apart. The ridges consist of fine sands with broken Bivalve and Gastropod shells with some Brachiopods and whale bones. In some parts of the Bay, near San Sebastian, there are as many as 17 parallel ridges (Fig. 2).

They are separated by washover channels that feed washover fans consisting of sandy-mud and shell debris (Fig. 9B). The ridges are densely vegetated by *Lepidophyllum* shrubs and Gramineae (Figs. 10B and 11). They have been interpreted as cheniers (Vilas and Arche, 1987), and can be considered as a special type of ‘chenier build by wave action’, as described by Augustinus (1989). Present notable differences with the classic examples of Louisiana, USA (Gould and McFarlan, 1959), Surinam (Wells and Coleman, 1981; Rine and Ginsburg, 1985; Augustinus et al., 1989) or the Gulf of Carpentaria, Australia (Rhodes, 1982; Chappell and Gindrod, 1984).

Thirteen samples of gastropod shells (Table 1) from different chenier ridges were dated by means of C-14 method ranging from 5270 ± 190 years (5116 ± 282 Cal BP) for the oldest, 7 km from the present day shoreline, to 910 ± 75 (509 ± 41.5) for the youngest, near the high-water mark were obtained (Fig. 2 profiles 1 and 2 and Fig. 15).

Table 1

Radiocarbon age determination from cheniers shell samples corresponding with Fig. 16

Sample no.	Material dated	Age BP ^a ¹³ C (corrected)	Error BP (±1 σ)	Calendar age ^b CalBP (±1 σ)
<i>Profile 1</i>				
GX-13293	shell	975	120	544(±83.5)
GX-13300	shell	1320	90	880(±94.5)
GX-13301	shell	1660	65	1221(±62)
GX-13299	shell	2595	80	2290(±95.5)
GX-13302	shell	3195	160	2966(±217)
GX-13303	shell	3700	85	3601(±109)
GX-13304	shell	4070	90	4084(±132.5)
<i>Profile 2</i>				
GX-13305	shell	910	75	509(±41.5)
GX-13294	shell	1755	120	1286(±107)
GX-13295	shell	2970	140	2736(±123.5)
GX-13296	shell	3505	150	3367(±171.5)
GX-13297	shell	4145	90	4202(±133.5)
GX-13298	shell	5270	120	5616(±282)

Calibrated ages of the original dates are shown for comparison.

^aG.L. No. 042461845.

^bStuiver and Reimer, 1993.

4.2.2. The upper intertidal zone

This is a flat, mudcracked area, 1.2 km wide. The sediments consist of alternating laminated and massively-bedded mud with transported Bivalve and Gastropod shells and some whale bones. Fine sand content increases to 10% seawards.

Allochthonous invertebrate faunas carried by waves and tides from the nearby shelf consist of rich assemblages of molluscs and some brachiopods. The most frequent gastropods are *Dontocymbiola magellanica*, *Adelomelon ancilla*, *Trophon geversianus*, *Trophon* sp., *Natica atrocyanea*, *Bucinanops* sp. and *Tegula* sp. and the most frequent bivalves are: *Aulacomya ater*, *Mytilus platensis*, *Darina solenoides* and *Vernus* sp.

4.2.3. The lower intertidal zone

This area is about 2.5–2.8 km wide. Sand content increases seaward and fine sands are dominant in the lower 0.8 km. The characteristic sedimentary structures are parallel rills of V-shaped section, 0.4–0.5 m wide, 0.4 m deep with narrow (0.3–0.6 m) inter-rill areas (Fig. 12). The rills evolve from tide-pools by wind-wave erosion as described above. A similar process has been described by Augustinus (1978). The rills do not migrate laterally, in contrast with the tidal channels, and become infilled by mud with linsen bedding and a basal lag of vertically stacked bivalve shells and clay chips. The inter-rill deposits consist of well laminated mud usually bioturbated by polychaete worms.

4.2.4. The sedimentary sequence

The composite sedimentary sequence for this area is very distinctive (Fig. 9A). Lenticular chenier deposits overly laminated to massively-bedded mud with mud cracks and abraded shells. These give way down section into well-laminated to bioturbated mud with concave scars infilled by a lag of bivalve shells, clay chips and mud with current ripples and linsen bedding. Laminated fine to very fine sandy with same abraded shells characterise basal deposits.

4.3. The gravel beaches and tidal flats near San Sebastian (Fig. 2, Zone D)

This area is about 8 km long, 34 km² in area from the mouth of the San Martin River to Punta Basilica

(Fig. 12). There are three main depositional environments in this area: a gravel and sand beach, a mixed tidal flat and a channelled area associated with the mouth of the San Martin River.

The beach exhibits several gravel ridges radiating from Punta Basilica, all with a recurved hook at the NW end. The ridges have a storm berm on top and a foreshore slope inclined at 24°–29° that is in sharp contact with the adjacent mudflat which slope away at 1°–3°. The berms include accumulations of shell debris and fish and whale bones.

There is a clear coarsening-upwards grain size distribution, from a maximum size of 3.5 cm at the base to 28 cm at the ridge crest berm. The beach is presently prograding over the mudflat. The gravel is derived from the rocky coastline to the SE, where the Miocene Carmen Silva Fm. lies covered by Quaternary tills, forming cliffs up to 55 m high. Based on a field experiment in the area, pebbles eroded from these cliffs move towards the NW under wave action at a rate of up to 14.5 m in 24 h.

The backshore dips landwards and is covered by eolian sands, colonised by Gramineae and other shrubs. A rodent, *Ctenomys* sp. excavates tunnels in the sand searching for the root that is its staple food.

The mixed tidal flat is the lateral equivalent of the rilled mudflats to the north of the Bay but contains a much higher percentage of sand due probably to the increased wave energy in a more open environment. Most of the mud deposited during calm periods is resuspended during storms and flaser bedding is frequent only near the beach. There are also thin clean gravel beds intercalated in the sands, deposited during severe storms. A few polychaete worms have been found in the northwestern part of the area.

The San Martin River is the only permanent river of the area, although it is very small and carries very little suspended load. The channel is highly sinuous and shows estuarine behaviour from the mouth to at least 3 km inland; tidal influence causes reversals of the currents and saline water intrusions.

The sedimentary sequence inferred for this area (Fig. 13) consist of three parts: (1) the sand-gravel beach at the top, about 3 m thick lying on an erosive surface and capped by a thin veneer of aeolian deposits; (2) the tidal flat mud with linsen and flaser bedding; and (3) the basal channel deposits at the mouth of the San Martín River.

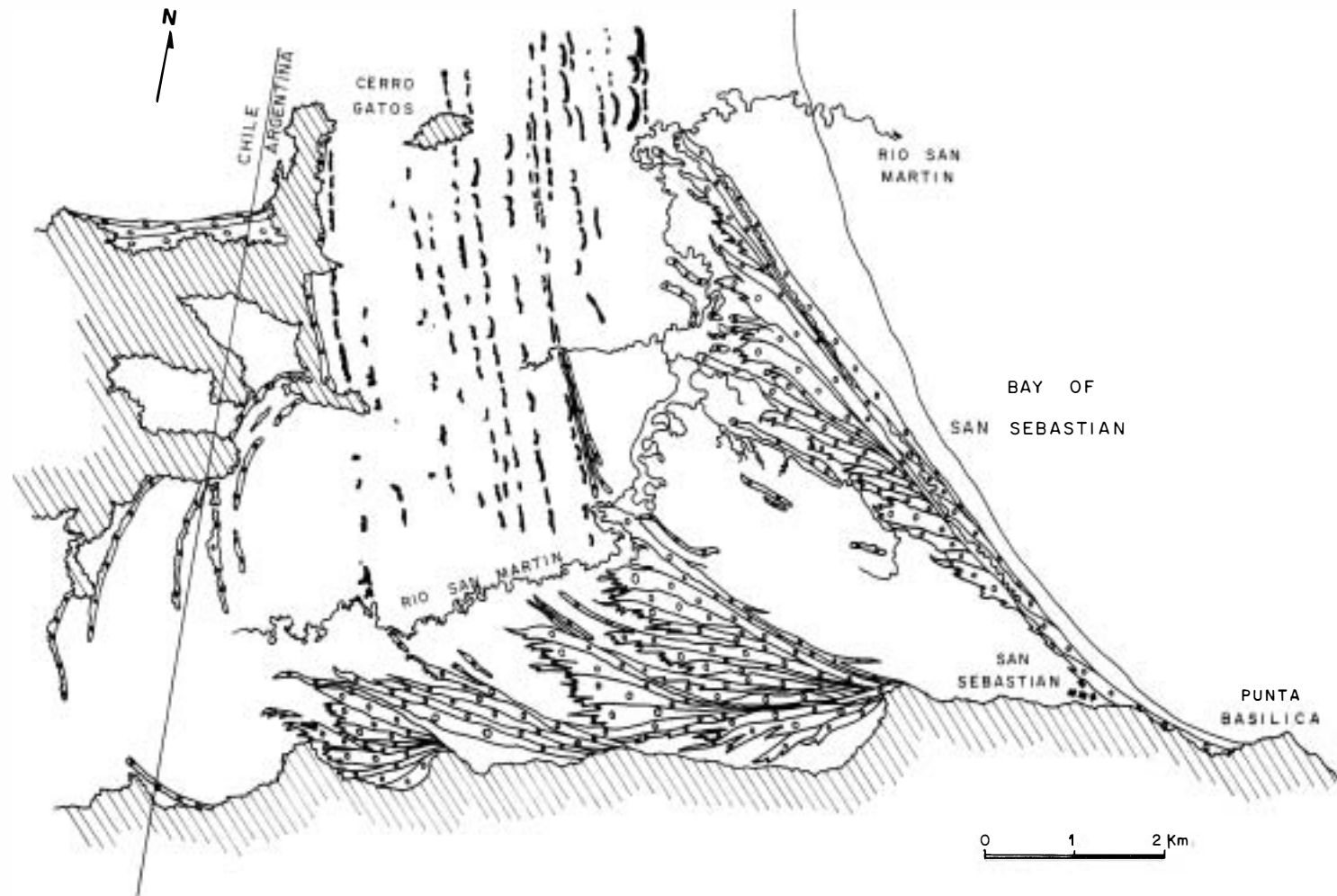


Fig. 12. Gravel beach complexes in the San Sebastian area. Note the fan-like shape of the beach ridges attached to capes along the paleocliff at the southern margin of the Bay. Ruled areas are highlands of Miocene rocks. Black lineaments are chenier ridges.

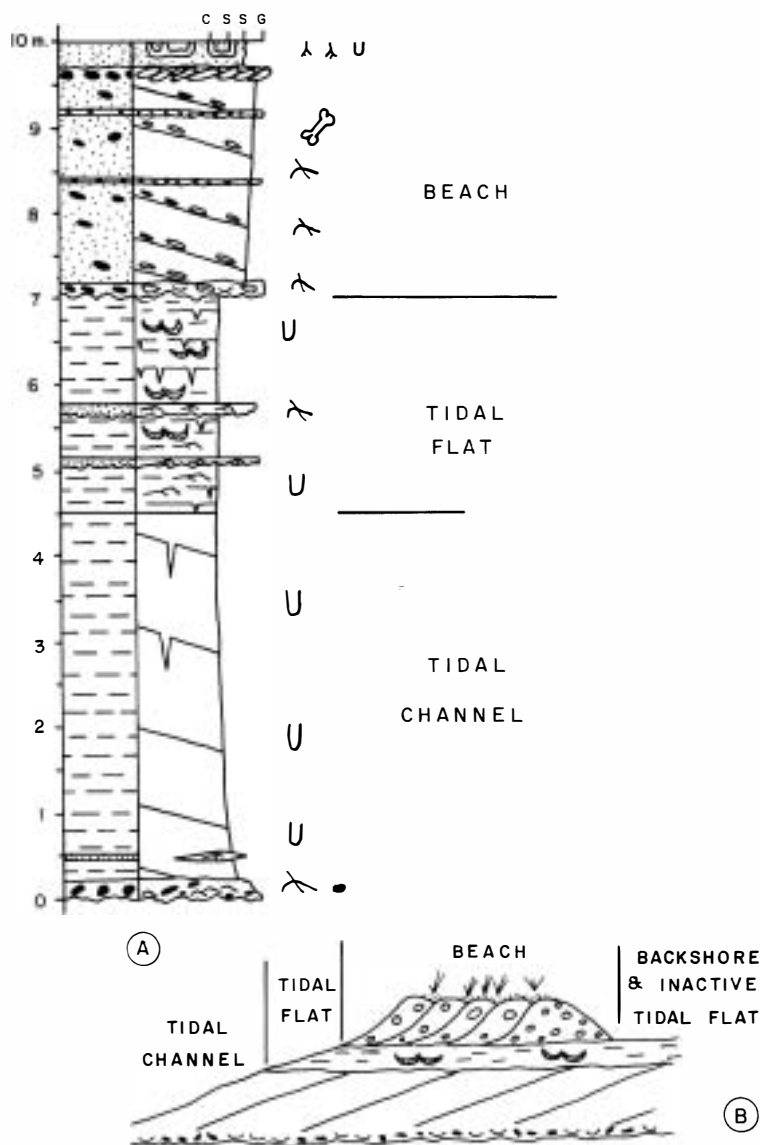


Fig. 13. (A) Beach-tidal flat sequence. (B) Progradation of the beach ridges that forces the tidal channels to migrate laterally. For legend see Fig. 8.

4.4. The cliffs east of Punta Basilica

The area (Fig. 2, Zone E) is about 5 km long; it is an erosive coast with high cliffs cut in the Miocene Carmen Silva Fm., and Quaternary tills. During low water a wide abrasion surface characterised by large rounded boulders and coarse sand patches is exposed, dipping seawards at 1° – 3° .

Different types of Bryozoa have been found covering the large boulders at the base of the San

Sebastian-Punta Basilica intertidal zona, and the Amphipod *Talitrus* sp. populates the sands at the base of the intertidal zone north of San Sebastian.

4.5. The beach-lagoon complex of Chorrillos

The beach-lagoon complex (Fig. 2, Zone F), is exposed to swell waves and consists of a gravel-sand

barrier beach trending E–W and an almost infilled lagoon. The complex is 9 km long, from Punta

Basilica to Cape San Sebastian, and almost 1.2 km wide near its eastern limit (Fig. 2).

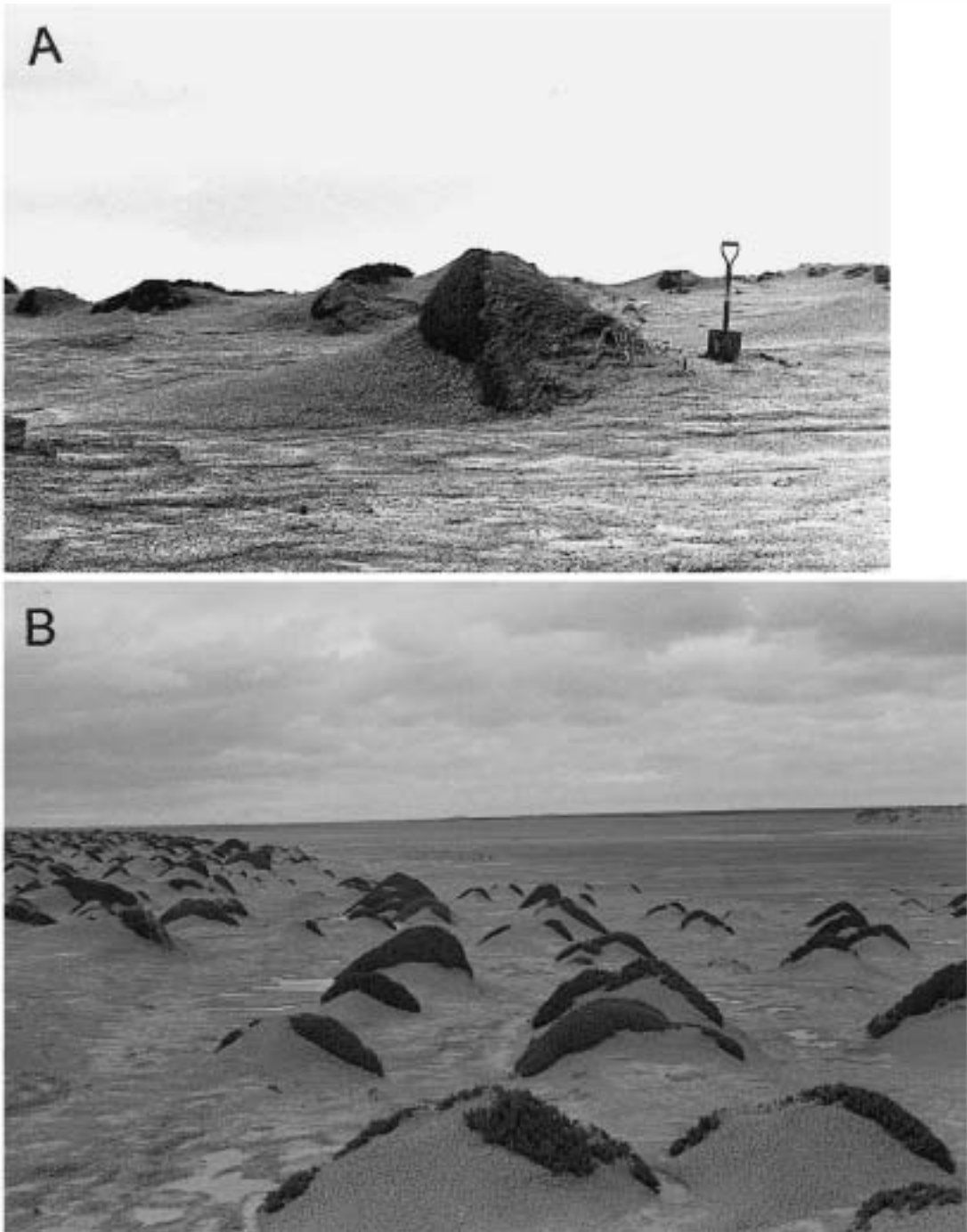


Fig. 14. Two types of clay dunes in the Cerro Redondo area (A) Comet-shaped, (B) Hemispherical or coppice dunes.

The beach is prograding over an abrasion platform cut in Quaternary tills, and consists of coarsening-upwards gravels with an abundant coarse sand matrix. Transport of the sediments is from W to E, forming parallel beach ridges.

The lagoon lies close to the Chorrillos cliff and is almost infilled by fine grained sediments with parallel lamination and wave ripples. The final infilling stage is the formation of extensive freshwater peats and related vegetation.

5. Eolian processes and deposits

The area west of the present day coastline (Fig. 2, zone G) consist of fossil supra- and intertidal sediments of Holocene age. The strong west wind removes grass cover leaving small, bare depressions. Rainwater collects in them during spring and summer and the wind creates wavelets that erode the eastern shore, enlarging the pond. During the dry season, deflation deepens the hollow and halite crusts form. After several seasons, a shallow temporal lake is created with a flat bottom. As deflation progresses, the water table is eventually reached, the vertical excavation ceases but the shore retreat continues. The lakes thus migrate to the east evolving a comet-like shape and may coalesce, forming large, complex depressions up to 4 × 15 km.

Eolian sediments form dust devils and clouds of silt-sized particles that are transported offshore several tens of kilometers and dumped into the Atlantic Ocean. Indurated silt pellets, 1–3 mm in diameter, are transported by saltation and accumulate around obstacles such as boulders or plants (Arche and Vilas, 1987).

Two types of coppice or clay dunes are formed (Fig. 14). Elongated dunes are usually found behind a *Lepidophyllum* plant, parallel to the prevailing wind, and may form extensive migrating fields. Hemispherical dunes are formed around *Sedum* plants and grow only vertically. When the plant dies, the dune is partially eroded by the wind and the sediments are deposited in extensive aeolian blankets beyond the dunefields. Rain percolates through the sediments destroying the original pellet leaving an homogeneous mass.

6. Discussion

6.1. Beach-ridge fan complexes and chenier ridges

The Chilean sector of Tierra del Fuego includes a coastal embayment now infilled by supra- and intertidal sediments, but well above present sea level. Two paleocliffs, trending roughly E–W, limited the ancestral bay, and some former stacks (rack formations) can be recognised.

Near San Sebastian (Fig. 12) there are four fan-shaped gravel beach ridge complexes along a paleocliff roughly trending E–W. The waves were reflected around coastal promontories and linear beach ridges accumulated until the coastline was smoothed. As infilling and progradation proceeded waves returned around the next seaward promontory and gave rise to a beach ridge 'fan complex', infilling the next embayment (Fig. 12).

The beach ridges pass laterally to the north into a series of linear chenier ridges. Radiocarbon dating of the shells found in them show they started to form at least 5200 years ago. The interchenier areas are filled by muddy supratidal saltmarsh and eolian sediments and muddy intertidal sediments are partially exposed in the shallow deflation lakes.

Chenier ridges die out to the north, probably due to the sheltering effect of the Península del Páramo spit and only muddy supratidal and intertidal sediments are found associated to some gravel beach ridges orientated E–W, parallel to the northern paleocliff.

The inactive part of the tidal complex is to a great extent covered by eolian deposits described elsewhere in this paper (Fig. 14). This blanket fossilizes the mudflat deposits and chenier ridges and assures its preservation, but observations and sampling of this area is possible only in the shallow deflation lakes during the dry summer period.

7. Comparison with other macrotidal environments

As mentioned above, there are some well known macrotidal complexes in the world: North Sea, Bay

of Fundy, China Sea, etc., but San Sebastian Bay differs from them in some important aspects.

In San Sebastian Bay grain size changes very little across the intertidal zone and sand content rarely exceeds 30%. Although the classic terms 'upper', 'middle' and 'lower intertidal zones' are employed in this paper, they do not mean mudflat, mixed flat and sandflat as in the North Sea and Bay of Fundy examples (see Reineck, 1963). In place of a 'granulometric' classification criteria, we suggest a geomorphic classification, with an upper flat area, middle tidal pool area and a lower tidal channel area. This lack of significant grain size gradient is by no means unique, because the tidal flats of China (Wang, 1983; Ren, 1986), Korea (Frey et al., 1988, 1989), Surinam (Rine and Ginsburg, 1985) and Australia (Rhodes, 1982) are also muddy and homogeneous.

Another difference with the classical areas is the geometry and dynamics of the tidal channels. Tidal channel bodies are a minor component of the North Sea tidal sediments and form lenticular bodies with large current structures. Tidal channels in the Bay of San Sebastian are straight, not sinuous, and migrate laterally forming point bar-like facies associations devoid of large current structures.

Faunas are also very different. Temperate tidal flats have high organic productivity with well known vertical changes in bivalve and gastropod communities. These invertebrates are absent from the San Sebastian intertidal area, where only a species of polychaete worm thrives. The juvenile forms live in the upper intertidal zone and the mature forms in the middle and lower zones.

Temperature is, perhaps, the key factor as the area is frozen for long periods in winter and this seldom happens in the more temperate North Atlantic areas.

Storm-related erosive scars and graded shell beds are frequent in the North Atlantic tidal complexes but they are absent in San Sebastian Bay. Substantial resuspension takes place during storms, but no characteristic storm beds have been identified. The cohesive nature of the muddy sediments prevents total reworking, even under a high-energy wave regime, and the subantarctic winter conditions, when most of the intertidal flat is frozen and covered by sea-ice fragments. The ice cover enhances the preservation potential of the sediments even during this stormy period.

The source of sediments is also different. Most macrotidal flats and chenier plains studied in other parts of the world receive most of their silt-clay fraction from river discharging in nearby areas (i.e., the China, Korea, Surinam, Australia, or Louisiana cases mentioned before). In San Sebastian Bay, however the source of the sediment is the wave erosion of coastal cliffs to the south and (to a lesser degree) north.

The closest comparison of San Sebastian Bay sediments can perhaps be made with the Taizhou Bay and Wenzhou area of Zhenjiang, China (Ren, 1986; Wang and Eisma, 1988). In these examples there are cheniers in the supratidal areas formed by shell debris derived from rapid mud sedimentation in the intertidal zone. Although the mud is of fluvial origin, there are very small vertical grain size changes, parallel lamination is the dominant internal structure and numerous parallel small tidal channels occur similar to the San Sebastian rills, but this spur-and-groove structure is of tidal, not wind wave origin, as in our case.

The progradation rates of San Sebastian Bay (0.6–2.1 mm/yr) are comparable with the figures for NW France (0.1 mm/yr) and Holland (4.9 mm/yr) and smaller than those for Turmagin Am, Alaska (12 mm/yr) and Wenzhou Bay, China (10 mm/yr) (de Klein, 1985; Wang and Eisma, 1988).

The cold climate of Tierra del Fuego is another characteristic control on sedimentation. Ice crystal marks on the mud control the mudcrack pattern and clay chip production. Pebble clusters have been found on the mud flats, interpreted as ice-rafted deposits. Some of these features were described for the Canadian Arctic coasts by Dionne (1988), but icepush ridges, ribbed grooves and other ice action marks are absent in San Sebastian Bay.

Finally, a peculiar feature of the San Sebastian Bay intertidal flat is the presence of numerous parallel rills controlled by the strong west wind and not by the slope of the flat.

8. Post-glacial evolution of the area

The San Sebastian Bay has been an area of net sedimentation since the last major advance of the Patagonian glaciers in the area, some 16,500–12,000

years ago (Caldenius, 1932; Raedecke, 1978; Porter et al., 1984; Heusser and Rabassa, 1987), that carved a paleovalley several tens of meters deep. It was drowned by a marine transgression and the relative sea level stabilised about 7000 years ago at its present position.

The glacio-isostatic rebound of the area, after the final retreat of the glaciers to the Andean high chain situated to the west of the Bay in this period caused a relative sea-level drop combined with a substantial rate of deposition. The continuous decrease in accommodation space, then, combines with the rapid accumulation of sediments to cause a forced regression of dual origin: tectonic and sedimentary.

The Holocene sedimentary record shows rapid coastal progradation and a relative sea-level drop of 8 m in the last 5200 years (Fig. 15). The oldest Holocene deposits have not been studied by us, so the date of initial sedimentation is unknown. On the southern Argentina coast, González and Weiler (1994) dated the maximum transgression peak at 5500–6000 years.

The ages of the chenier ridges have been obtained by C-14 dating of unabraded shells (Fig. 15). The muddy intertidal sediments contain very few shells, always broken and abraded and have not been dated directly. The chenier is clearly younger than the underlying mud.

The ages of the ridges (Fig. 15) show a seawards decreasing progradation rate, estimated at 2.35 m/yr in the beginning of the process and 0.6 m/yr at the end; these rates are comparable with the calculations

of Codignotto (1983) for the same area (about 1 m/yr) and with prograding tidal complexes in other part of the world such as 4.1 m/yr at Scheveningen, Holland, (Van Straaten, 1965), 1.4–2.8 m/yr for Nayarit, Mexico (Curry et al., 1969), 1.1 m/yr for the Louisiana Chenier Coast, USA (Coleman, 1966) and 1.6–4.8 m/yr for the Gulf of Carpentaria, Australia (Rhodes, 1982).

As the oldest chenier ridges and gravel beaches are now 8 m above high tide watermark (Fig. 15), the relative sea-level drop was caused probably by a glacio-isostatic rebound after the retreat of glaciers from the Bahía Inútil-San Sebastian Bay area. This started about 12,000 years ago and was completed around 7000 years BP (Raedecke, 1978). The relative sea-level drop is a regional phenomenon, and has not been observed in other areas of the Argentinean coastline.

Assuming that the rate of isostatic rise is decreasing with time, the chenier ridges and gravel beach ridges would be expected to become closer with time (given a constant slope and sediment supply rate).

The decreased progradation rate could be related a reduction of sediment supply (from cliffs surrounding the Bay). This, in turn, may result from the progradation of mudflats and growth of gravel beach ridges which shield the cliffs and reduce the effects of wave erosion. As deposition progrades into the deepest parts of the ice-carved paleovalley there is an increase in accommodation space; if the sedimentation rate was constant with time, then the progradation rate will decrease with time (Fig. 16).

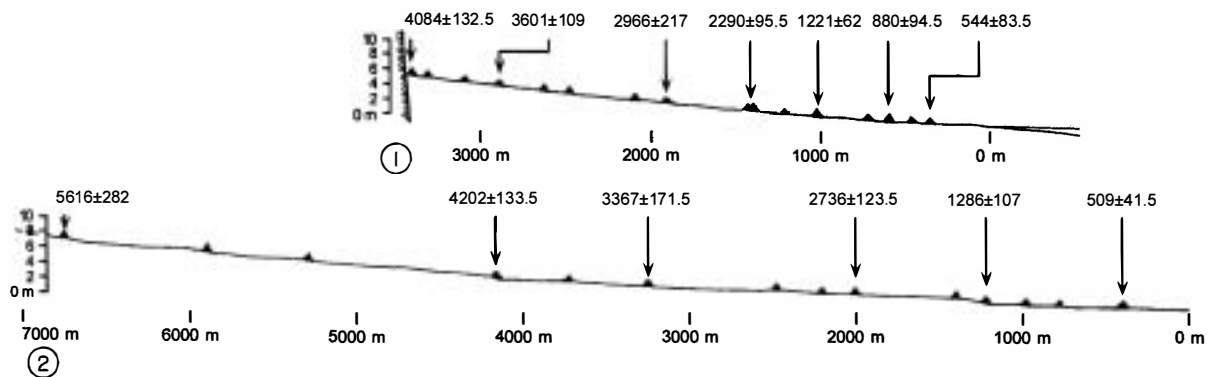


Fig. 15. Radiocarbon ages of the Chenier ridges in two transects (1 and 2, see Fig. 2 and Table 1).

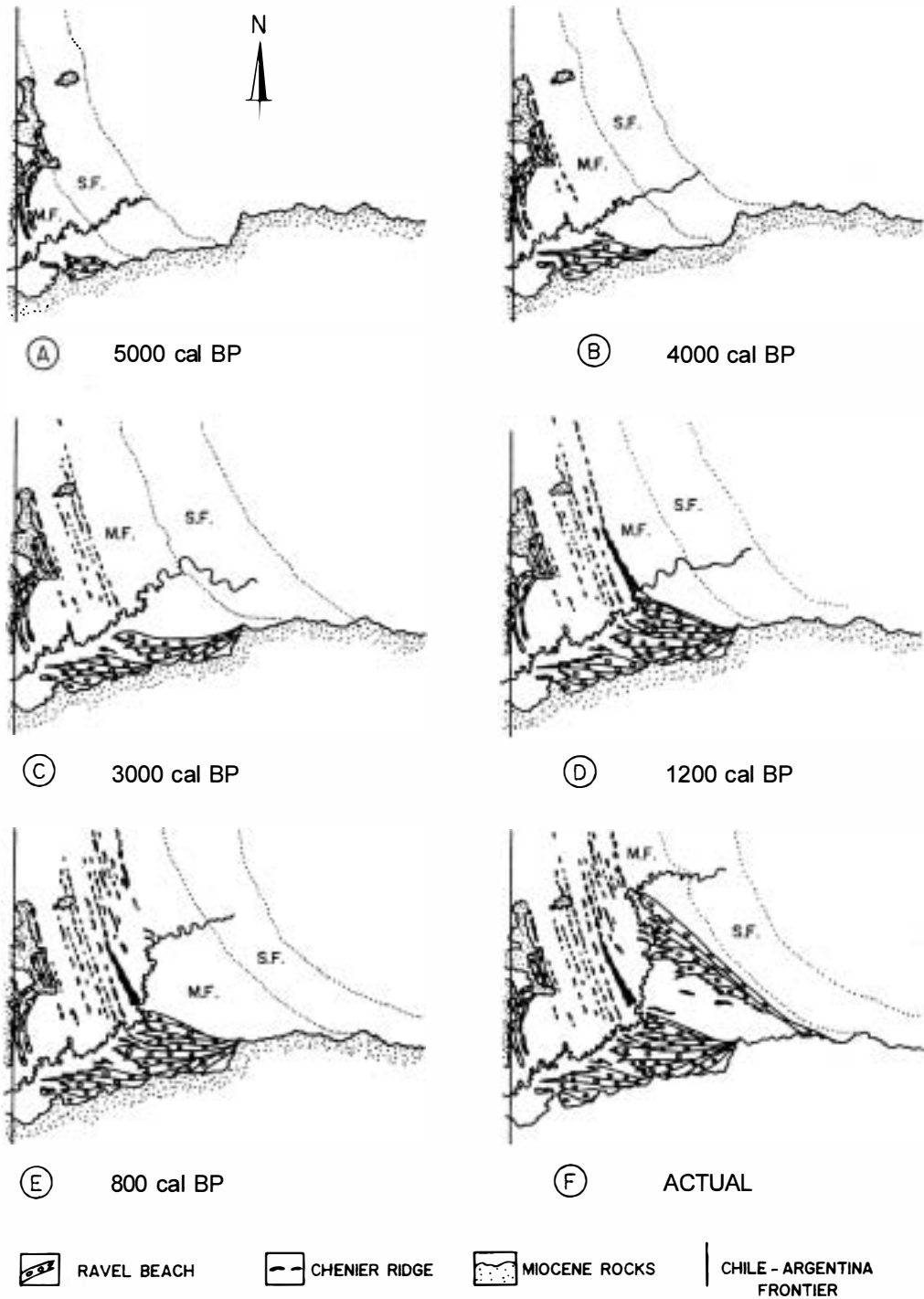


Fig. 16. Evolution of the SW part of San Sebastian Bay since approximately 5000 years cal BP. Different stages from A to F, represents the growth of gravel beach ridges, mud flats and cheniers ridges, after the Holocene transgression.

9. Conclusions

–San Sebastian Bay is a high-energy coastal embayment with active sedimentation since the last glacial stage, controlled by waves of local and Atlantic Ocean origin and tides with a range of up to 10.4 m. The sediments lie on a fluvio-glacial paleo-valley cut into Miocene and Quaternary sediments, partially drowned by the last Holocene transgression.

–Sedimentation takes place in wave-dominated environments (Peninsula del Páramo, San Sebastian and Chorrillos gravel beaches), tide-dominated environments (muddy tidal flats) and mixed-influence environments (cheniers and inter-chenier areas).

–San Sebastian Bay is a marine tidal complex, without any river influence, in contrast to the better known estuarine macrotidal complexes.

–Extensive muddy tidal flats, with strong wind control on the intertidal sedimentation, are deposited with a non-channelled lower part with planar or trough cross bedding that is really a series of accretion surfaces. The secondary tidal channels have high sinuosity but the main ones are straight. Capture processes are frequent.

–The clay mineralogy of the tidal deposits has permitted identification of the Miocene outcrops along the southern margin of the Bay as the main sediment source, excluding the tills cropping out along the northern margin as a major source area.

–Although the Bay is a high energy environment, the internal structures of the sediments are only parallel lamination and wave and current ripples, due to the cohesive nature of the sediments. Bioturbation is abundant only in the lowest part of the complex and is caused by a single species of polychaete worm, the only fauna present.

–The chenier ridge deposits are formed by storms that carry shell debris from the shelf. The resulting linear ridges are fixed afterwards by vegetation and a thin aeolian silt layer.

–The oldest part of the complex is now under intense deflation that forms extensive shallow lakes and deposition of an eolian blanket of mud pellets with pseudo-trough cross bedding.

–The Bay of San Sebastian is an area of active sedimentation and a progradation rate decreasing from 2.35 m/yr to 0.6 m/yr from the last 5000 years.

Acknowledgements

We would like to thank our colleagues Dr. Gustavo G. Bonorino (Secretaría de Minas, Buenos Aires), Dr. Gustavo Bujalesky (C.A.D.I.C.), and Dr. Enrique Schnack (U. Mar del Plata) for their help during field campaigns and discussion of the results. We also thank Dr. Jorge Rabassa, Director of the C.A.D.I.C., Ushuaia, for his help with accommodation, transport and logistics, the personnel of the Gendarmería Nacional and Policía Territorial in San Sebastian and Cuyen for fieldwork support, and Mr. Oscar Zanola, Director of the Museo Territorial. The C.S.I.C. (Spain) and C.O.N.I.C.E.T. (Argentina) made possible this project under their collaboration agreements, and the C.A.Y.C.I.T. (Spain) agreed to include it in its program 1378/82. Thanks to Ana Dorato (C.A.D.I.C.) for figure drafting, Piedad Martín for typing the first manuscript, and G. Frances, S. Garcia-Gil and P. Diz (UVI) for their help in the last version. Thanks to Harold G. Reading, (U. Oxford UK), Dr. Robert W. Frey (U. Georgia USA) and Dr. Bruce S. Hart (Pacific Geoscience Centre, Sydney, Canada) who read a first version of the manuscript and made numerous observations. Thanks to P.T. Harris (U. Tasmania), P.G.E.F. Augustinus (U. Utrecht) and one anonymous reviewer for their comments and observations which greatly improved the manuscript.

References

- Allen, J.R.L., 1987. Late Flandrian shoreline oscillations in the Severn Estuary: the Rumney Formation at its typesite (Cardiff Area). *Phil. Trans. R. Soc. London B* 315, 157–174.
- Allen, J.R.L., 1988. Modern-period muddy sediments in the Severn Estuary (Southwest UK) a pollutant-based model for dating and correlation. *Sediment. Geol.* 58, 1–21.
- Allen, J.R.L., 1990. The Severn Estuary in southwest Britain: its retreat under marine transgression and fine sediment regime. *Sediment. Geol.* 66, 13–28.
- Amos, C.L., Buckley, D.E., Doborn, G.R., Dalrymple, R.W., M. Cann, S.B., Risk, M.J., 1980. Geomorphology and sedimentology of the bay of Fundy. *Guidebook Geol. Assoc. Canada*, Annu. Meeting, Halifax, Trip 23, 82 pp.
- Arche, A., Vilas, F., 1987. Depósitos eólicos de grano fino en la Bahía de San Sebastian Tierra de Fuego, Argentina. *Acta Geol. Hisp.* 21–22, 261–266.

- Augustinus, P.G.E.F., 1978. The changing Shoreline of Surinam (South America), PhD Thesis. Utrecht University, 232 pp. (pp. 201–202).
- Augustinus, P.G.E.F., 1989. Cheniers and Chenier plains: a general introduction. *Marine Geology* 90, 219–229.
- Augustinus, P.G.E.F., Hazelhoff, L., Kroon, L., 1989. The chenier coast of Suriname: modern and geological development. *Marine Geology* 90, 269–281.
- Avoine, J., 1986. Sediment exchanges between the Seine estuary and its adjacent shelf. *J. Geol. Soc. London* 144, 135–148.
- Avoine, J., Larssonneur, C., 1987. Dynamics and behaviour of suspended sediment in macrotidal estuaries along the south coast of the English Channel. *Continental Shelf Res.* 7, 1301–1305.
- Beeftnik, W.G., 1977. Salt marshes. In: Barnes, R.S.K. (Ed.), *The Coastline*, Wiley, pp. 93–122.
- Bujalesky, Q., González Bonorino, G., Arche, A., Isla, F., Vilas, F., 1987. La espiga peninsula Páramo, Isla Grande de la Tierra del Fuego, Argentina. *Congr. Geol. Arg., X. Arg. Geol. Assoc., Tucumán*, pp. 115–117.
- Caldenius, C.C., 1932. Las glaciaciones cuaternarias en la Patagonia y Tierra del Fuego. *Geogr. Ann.* 14, 1–164.
- Codignotto, J.O., 1979. Hojas geológicas 63a, Cullen, 64a, San Sebastian y 65b Rio Grande. Servicio Geológico nacional, Argentina.
- Codignotto, J.O., 1983. Depósitos elevados y/o de acreción Pleistoceno–Holoceno en la costa Fueguino-Patagónica. *Simp. Osc. del nivel del mar durante el último hemicycle de glacial en la Argentina. Mar del Plata, Argentina*, pp. 12–26.
- Codignotto, J.O., Malumian, N., 1981. Geología de la región al Norte del paralelo 54°S de la Isla Grande de la Tierra del Fuego. *Rev. Ass. Argentina Geol.* 36, 44–88.
- Coleman, J.M., 1966. Recent Coastal Sedimentation: central Louisiana coast. *State Univ. Coastal Stud. Inst., Tech. Report* 29, 1–73.
- Curray, J.R., Emmel, F.J., Crampton, P.J.S., 1969. Holocene history of a strand plain, Nayarit, Mexico. *Lagunas Costeras, un Simposio, UNAM-UNESCO Mexico*, pp. 61–100.
- Chappell, J., Gindrod, J., 1984. Chenier Plain formation in Northern Australia. In: Thom, B.G. (Ed.), *Coastal Geomorphology of Australia*, Academic Press, pp. 197–231.
- Dalrymple, R.W., Knight, R.J., Zaitlin, B.A., Middleton, G.V., 1990. Dynamics and facies model of a macrotidal sand-bar complex, Cobequid Bay-Salmon River Estuary (Bay of Fundy). *Sedimentology* 37, 577–612.
- Dionne, J.C., 1988. Characteristic features of modern tidal flats in cold regions. In: De Boer, P.L. (Ed.), *Tide-Influenced Sedimentary Environments and Facies*, Reidel, pp. 301–332.
- Evans, G., 1965. Intertidal flat sediments and their environments of deposition in the Wash. *Q. J. Geol. Soc. London* 121, 209–245.
- Frey, R.W., Basan, P.B., 1985. Coastal salt marshes. In: Davis, R.A., Jr. (Ed.), *Coastal Sedimentary Environments*, Springer, pp. 225–301.
- Frey, R.W., Hong, J.S., Hayes, W.B., 1988. Physical and biological aspects of shelf accumulation on a modern macrotidal flat, Inchon, Korea. *Neth. J. Sea Res.* 22, 267–278.
- Frey, R.W., Howard, J.D., Han, S.J., Park, B.K., 1989. Sediments and sedimentary sequences on a modern macrotidal flat, Inchon, Korea. *J. Sediment. Petrol.* 59, 28–44.
- González, M.A., Weiler, N.E., 1994. Argentina Holocene Transgression: Sidereal Ages. *J. Coastal Res.* 10, 621–627.
- Gould, H.R., McFarlan, E., 1959. Geological history of the Chenier Plain, southwestern Louisiana. *Trans. Gulf Coast Ass. Geol. Soc.* 9, 261–270.
- Harris, P.T., Collins, M.B., 1985. Bedform distributions and sediment transport patterns in the Bristol Channel and Severn Estuary, U.K. *Mar. Geol.* 62, 153–166.
- Heusser, C.J., Rabassa, J., 1987. Cold Climate episode of Younger Dryas age in Tierra del Fuego. *Nature* 328, 609–611.
- Isla, F.I., 1993. Overpassing and armouring phenomena on gravel beaches. *Mar. Geology* 110, 369–376.
- Isla, F.I., Vilas, F., Bujalesky, G.G., Ferrero, M., González-Bonorino, G., Arche, A., 1991. Gravel drift and wind effects on the macrotidal San Sebastian Bay, Tierra del Fuego, Argentina. *Mar. Geol.* 97, 211–224.
- Kirby, R., Parker, W.R., 1982. A suspended sediment front in the Severn Estuary. *Nature* 295, 396–399.
- de Klein, G.V., 1985. Intertidal flats and intertidal sand bodies. In: Davis, R.A., Jr. (Ed.), *Coastal Sedimentary Environments*, Springer, pp. 187–224.
- Knight, R.J., Dalrymple, R.W., 1975. Intertidal sediments from the south shore of Cobequid Bay, Bay of Fundy, Nova Scotia, Canada. In: Ginsburg, R.N. (Ed.), *Tidal Deposits*, Springer, pp. 47–55.
- Larssonneur, C., 1982. La Baie du Mont-Saint-Michel: un modèle de sédimentation en zone tempérée. *Rev. Palais Decouverte* 10, 50–69.
- Pejrup, M., 1988. The triangular diagram used for classification of estuarine sediments, a new approach. In: De Boer, P.L., Van Gelder, A., Nio, S.D. (Eds.), *Tide-Influenced Sedimentary Environments and Facies*, Reidel, pp. 289–300.
- Porter, S.C., Stuiver, M., Heusser, C.J., 1984. Holocene sea-level changes along the Strait of Magellan and Beagle Channel, southernmost South America. *Quat. Res.* 22, 58–67.
- Raedecke, L.D., 1978. Formas del terreno y depósitos cuaternarios, Tierra del Fuego Central, Chile. *Rev. Geol. Chile* 5, 3–31.
- Reineck, H.E., 1958. Wühlban-Gefüge in Abhängigkeit von sediment Umlagerungen. *Senckenbergiana Lethaea* 39, 1–56.
- Reineck, H.E., 1963. Sedimentgefüge in Berich der Sudliche Nordsee. *Abh. Senckenberg Nat. Gesell.* 505, 1–138.
- Reineck, H.E., 1972. Tidal Flats. *Spec. Publ.-SEPM* 16, 146–159.
- Ren, M.-E., 1986. Tidal mud flats. In: Ren, M.-E. (Ed.), *Modern Sedimentation in the Coastal and Nearshore Zones of China*, Springer, pp. 78–145.
- Rhodes, E.G., 1982. Depositional model for a Chenier plain, Gulf of Carpentaria, Australia. *Sedimentology* 29, 201–222.
- Rine, J.M., Ginsburg, R.N., 1985. Depositional facies of a muddy shoreface in Surinam, South America. *J. Sediment. Petrol.* 55, 633–652.
- Rutter, N., Schnack, E.J., Del Rio, J., Fassano, J.L., Isla, F.I., Radke, U., 1989. Correlation and dating of Quaternary Littoral zones along the Patagonian coast, Argentina. *Quat. Sci. Rev.* 8, 213–234.

- Servicio de Hidrografía Naval, 1987. Corrientes de marea en Tierra del Fuego (Bahía de San Sebastian), inédito.
- Servicio de Hidrografía Naval, 1988. Tabla de mareas para 1988. Puertos de la R. de Argentina. Armada Argentina. Publicación H-610.
- Servicio de Meteorológico Nacional, 1986. Estadísticas meteorológicas (1971-1980). Fuerza Aérea Argentina. Estadística no. 36.
- Van Straaten, L.M.J.V., 1965. Coastal barrier deposits in south and north-Holland. *Meded. Geol. Sticht.* 17, 41-75.
- Stuiver, M., Reimer, P.I., 1993. Extended 14-C database and revised CALIB radiocarbon calibration program. *Radiocarbon* 35, 215-230.
- TOTAL AUSTRAL-GEOMATTER, 1980. Geophysical and geotechnical soil survey, offshore Tierra del Fuego, Argentina. Unpublished report.
- Vilas, F., Arche, A., 1987. Llanura de Cheniers en la Bahía de San Sebastian, Tierra del Fuego, Argentina. *Acta Geol. Hisp.* 21-22, 535-539.
- Vilas, F., Arche, A., Ferrero, M., Bujalesky, G.G., Isla, F.I., González-Bonorino, G., 1987. Esquema evolutivo de la sedimentación reciente en la Bahía San Sebastian, Tierra del Fuego, Argentina. *Thalassas* 5, 33-36.
- Wang, Y., 1983. The Mudflat system of China. *Can. J. Fish. Aquat. Sci.* 40 (1), 160-171.
- Wang, B.-C., Eisma, D., 1988. Mudflat deposition along the Wenzhou Coastal Plain in Southern Zhejiang, China. In: De Boer, P.L. (Ed.), *Tide-Influenced Sedimentary Environments and Facies*, Reidel, pp. 265-274.
- Wells, J.T., Coleman, J.M., 1981. Periodic mudflat progradation, northeastern Coast of South America: a hypothesis. *J. Sediment. Petrol.* 51, 1069-1075.